Chapter 3

Solution of Riemann problem for dusty gas flow

3.1 Introduction

In gasdynamics, Riemann problem is an initial value problem for the system of one dimensional Euler equations supplemented by a discontinuous initial data. Its solution consists of three waves, with the middle wave as a contact discontinuity and the other two waves are shock or rarefaction waves depending upon the initial data. Also, it gives us an idea of the wave structure of a system of hyperbolic partial differential equations. In recent decades solution of the Riemann problem for the Euler equations of ordinary gasdynamics has been analyzed extensively. Lax (1957) solved the Riemann problem by considering the difference between initial data, $\|V_L - V_R\|$, sufficiently small, where V_L and V_R are vectors of conserved variables at constant states separated by a discontinuity. Smoller (1969) presented a solution of the Riemann problem for an extended class of hyperbolic systems with V_L and V_R to be arbitrary constant vectors. Glimm (1965) used the solutions of Riemann problem in construction of a solution to the general initial value problem using the random choice method. Godunov (1976) and Chorin (1976) has proposed the exact solution of the Riemann problem, however, Smoller (1969) has proposed a different approach to determine the exact solution. Liu (1975) solved the Riemann problem for general system of conservation laws subject to entropy condition. Toro (1989), (1995) presented a Riemann solver for the exact

---

The contents of this chapter have been published in **IJNLM – International Journal of Non-Linear Mechanics**.

solution of the Riemann problem for ideal and covolume gases. Using the solution of the Riemann problem, Godunov (1959) presented a numerical scheme for the solution of a nonlinear system of hyperbolic conservation laws. As the Riemann problem does not admit a solution in closed form, even for ideal gas, many authors, such as Godunov (1959), Chorin (1976), Smoller (1969), Gottlieb and Groth (1988), Quartapelle *et al.* (2003) and Toro (2009), among several others, developed iterative methods for the solution to determine the flow field. Menikoff and Plohr (1989) studied the Riemann problem for fluid flow of real materials with arbitrary equation of state, subject to the physical requirements of thermodynamics like phase transition. Recently Shekhar and Sharma (2010), (2012), Singh and Singh (2014) presented the solution of Riemann problem for one dimensional magnetogasdynamics flow. Gupta and Singh (2015) used random choice method for the solution of dam break problem which is an example of Riemann problem for shallow water equations. A detailed discussion on the Riemann problem can be found in the books Smoller (1994), Toro (2009), Li (1994), Dafermos (2000), Bressan (2000) and LeVeque (2002). In the case of Euler equations Riemann problem contains the shock tube problem given in Sod (1978). To determine the exact closed form solution to the Riemann problem for the Euler equations is still an open problem.

The study of Riemann problem for the fluid flow containing solid particles is a subject of great interest both from mathematical and physical point of view due to its applications such as in underground explosions (Lamb et al. (1992)), interstellar mass flow (Laibe et al. (2014)) and explosive volcanic eruptions (Pelanti et al. (2006)) etc. Dusty gas is a mixture of gas and small solid particles where solid particles occupy less than 5% of total volume. When the speed of fluid is very high, the small solid particles behave like a pseudo fluid (Pai (1977)). Miura and Glass (1983) studied the flow resulting from the passage of a shock wave through a dusty-gas layer. The basics of gas particle flow can be found in Rudinger (1980). The dynamical behaviour of a fluid is governed by the principle of conservation of mass, momentum and energy. Here we consider a single fluid model for dusty gas. The present chapter aims to provide an approximate analytical solution to the Riemann problem for the one–dimensional, time–dependent Euler equations for dusty gas flow. In case both external waves are rarefaction waves then it might create vacuum in the solution of Riemann problem depending upon the initial data. Using the Riemann solver of Toro (2009) the non-vacuum solutions are determined, which is obtained if the pressure positivity condition is satisfied. It is also assessed as to how the presence of dust particles influences the solution across the shock wave, rarefaction wave and contact discontinuity.

3.2 Formulation of the problem

The governing equations describing a planar flow of a dusty gas mixture obeying the equation of state of Mie Grüneisen type

$$p = (1-k_p)\rho RT/(1-Z), \tag{3.1}$$

are given as (Pai, 1977), (Miura et al., 1983), (Rudinger, 1980) and (Pai et al., 1980)

$$\begin{aligned} &\rho_t + v\rho_x + \rho v_x = 0, \\ &\rho(v_t + vv_x) + p_x = 0, \\ &p_t + vp_x + \rho c^2 v_x = 0, \end{aligned} \tag{3.2}$$

where v is the particle velocity along x-axis, t is the time, ρ is the density, p is the pressure, T is the temperature and R is the gas constant. The entity $Z = V_{sp}/V_g$ is the volume fraction and $k_p = m_{sp}/m_g$ is the mass fraction of the solid particles in the mixture where m_{sp} and V_{sp} are the total mass and volumetric extension of the solid particles and V_g and m_g are the total volume and total mass of the mixture respectively.

The quantity

$$c = \left(\Gamma p / ((1-\theta\rho)\rho)\right)^{1/2}, \tag{3.3}$$

is the equilibrium speed of sound with

$$\Gamma = \gamma(1+\lambda\beta)/(1+\lambda\beta\gamma),\ \lambda = k_p/(1-k_p),\ \beta = c_{sp}/c_p,\ \gamma = c_p/c_v. \tag{3.4}$$

Here c_{sp} is the specific heat of the solid particles, c_p the specific heat of the gas at constant pressure, and c_v the specific heat of the gas at constant volume. The relation between the entities Z and k_p is given by $Z = \theta\rho$, $\theta = k_p/\rho_{sp}$, with ρ_{sp} as the species density of the solid particles.

The internal energy per unit mass of the mixture is given as

$$e = (1-Z)\,p/((\Gamma-1)\rho). \tag{3.5}$$

3.3 The Riemann problem and generalized Riemann invariants

The system of governing equations (3.2) along with (3.5) can be written in conservation form as

$$\left.\begin{aligned} &V_t + F(V)_x = 0, \\ &V = \begin{bmatrix} \rho \\ \rho v \\ E \end{bmatrix},\ F(V) = \begin{bmatrix} \rho v \\ \rho v^2 + p \\ v(E+p) \end{bmatrix}, \end{aligned}\right\} \tag{3.6}$$

where $E = \rho e + \rho v^2/2$.

The initial conditions for the Riemann problem are

$$V(x,0) = \begin{cases} V_L, \text{ if } x<0 \\ V_R, \text{ if } x>0 \end{cases}, \tag{3.7}$$

where $-\infty < x < \infty,\ t>0$. We can take x to vary in a finite interval $[x_L,\ x_R]$ around the point $x=0$. In the solution of Riemann problem, $U = (\rho, v, p)^T$ is taken as vector of primitive variables. The initial data of Riemann problem (3.6)-(3.7) consists of two constant states, which are $U_L = (\rho_L, v_L, p_L)$ to the left of $x = 0$ and $U_R = (\rho_R, v_R, p_R)$ to the right of $x = 0$, separated by a discontinuity at $x = 0$. Physically, with reference to Euler equations, the shock-tube problem may be generalized as Riemann problem consisting of two stationary gases $(v_L = v_R = 0)$ in a tube separated by a diaphragm. When the diaphragm is broken down suddenly it produces a nearly centered wave system consisting of a rarefaction wave, a contact discontinuity and a shock wave.

The hyperbolic system of equations (3.6) admits the following family of characteristics

$$dx/dt = v - c,\ dx/dt = v,\ dx/dt = v + c. \tag{3.8}$$

The family of characteristics given by second equation of (3.8) represents the particle path while those given by first and third represent the wave propagating in the negative and positive direction along x-axis, respectively. These three waves corresponding to equation (3.8) separate four constant states from left to right V_L, V_L^*, V_R^* and V_R. The unknown star region between the left and right waves is divided by the middle wave into two sub regions star left (V_L^*) and star right (V_R^*).

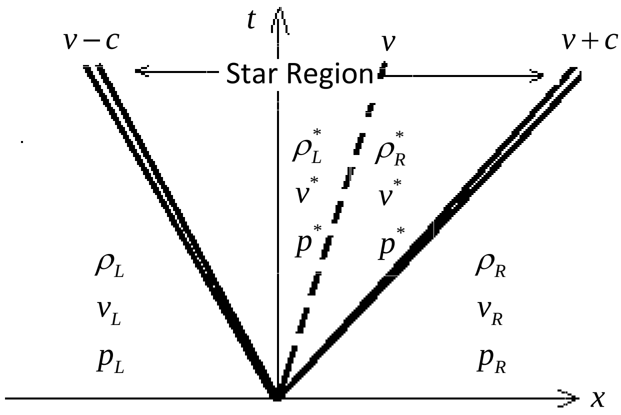

Figure 3.1 Structure of the solution of the Riemann problem for Euler equations

From the eigen structure of the Euler equations it can be easily seen that the middle wave is always a contact discontinuity while the left and right (nonlinear) waves are either rarefaction or shock waves. Thus according to the type of non-linear waves, there can be four possible wave patterns.

It can also be seen that both pressure p^* and particle velocity v^* are constant in the star region. Our solution procedure makes use of the constancy of pressure and velocity in the star region, see Toro (2009). For the isentropic case, we can replace the third equation by the entropy equation

$S_t + vS_x = 0$.

Then the system (3.6), can be written as

$$\begin{bmatrix} \rho \\ v \\ S \end{bmatrix}_t + \begin{bmatrix} v & \rho & 0 \\ c^2/\rho & v & (1/\rho)\partial p/\partial S \\ 0 & 0 & v \end{bmatrix} \begin{bmatrix} \rho \\ v \\ S \end{bmatrix}_x = \begin{bmatrix} 0 \\ 0 \\ 0 \end{bmatrix}.$$

The eigenvalues of the above system are

$\lambda_1 = v - c,\ \lambda_2 = v,\ \lambda_3 = v + c$,

and the corresponding right eigenvectors are

$$k^1 = \begin{bmatrix} 1 \\ -c/\rho \\ 0 \end{bmatrix},\ k^2 = \begin{bmatrix} -\partial p/\partial S \\ 0 \\ c^2 \end{bmatrix},\ k^3 = \begin{bmatrix} 1 \\ c/\rho \\ 0 \end{bmatrix}.$$

Across the wave associated with $\lambda_1 = v - c$, we have

$$\frac{d\rho}{1} = \frac{dv}{-c/\rho} = \frac{dS}{0},$$

which gives the relations

$dv + (c/\rho)d\rho = 0$ and $dS = 0$.

i.e., $v + \int (c/\rho) d\rho =$ constant and $S =$ constant.

Similarly, across the $\lambda_3 = v + c$, wave we have

$v - \int (c/\rho) d\rho =$ constant and $S =$ constant, which are the generalized Riemann invariants for the system of equations (6).

3.4 Equation for pressure and velocity

To compute the pressure p, velocity v in the star region we establish a proposition.

Proposition: The solution for pressure p^* of the Riemann problem (3.6) – (3.7) with the equation of state (3.1) for dusty gas is given by the root of the equation $f(p,V_L,V_R)=0$, with

$$f(p,V_L,V_R)=f_L(p,V_L)+f_R(p,V_R)+v_R-v_L, \tag{3.9}$$

where the function f_L is given by

$$f_L(p,V_L)=\begin{cases}(p-p_L)\left[A_L/(p+B_L)\right]^{1/2}, & \text{if } p>p_L \text{ (shock wave)},\\ 2c_L(1-\theta\rho_L)/(\Gamma-1)\left\{\left(p/p_L\right)^{(\Gamma-1)/2\Gamma}-1\right\}, & \text{if } p\le p_L \text{ (rarefaction wave)},\end{cases} \tag{3.10}$$

and the function f_R is given by

$$f_R(p,V_R)=\begin{cases}(p-p_R)\left[A_R/(p+B_R)\right]^{1/2}, & \text{if } p>p_R \text{ (shock wave)},\\ 2c_R(1-\theta\rho_R)/(\Gamma-1)\left\{\left(p/p_R\right)^{(\Gamma-1)/2\Gamma}-1\right\}, & \text{if } p\le p_R \text{ (rarefaction wave)},\end{cases} \tag{3.11}$$

and the data dependent constants A_L, A_R, B_L, B_R are given by

$$\left.\begin{aligned}A_L&=(1-\theta\rho_L)/(\rho_L(1+\Pi)), \quad B_L=\Pi p_L/(1+\Pi),\\ A_R&=(1-\theta\rho_R)/(\rho_R(1+\Pi)), \quad B_R=\Pi p_R/(1+\Pi),\end{aligned}\right\} \tag{3.12}$$

where $\Pi=(\Gamma-1)/2$.

The solution for the particle velocity v^* in the star region is

$$v^*=(v_L+v_R)/2+(f_L(p^*)+f_R(p^*))/2. \tag{3.13}$$

Once equation (3.9) is solved for p^*, velocity v^* can be found as in (3.13) and the remaining unknowns are found by using some standard relations of gasdynamics.

Proof: We derive the function f_L by considering the left wave as a shock wave and then a rarefaction wave. Similarly f_R is derived.

3.4.1 Left Shock Wave

Suppose that the left wave is a shock moving with speed G_L as shown in the Figure 3.1.

We transform the equations to a frame of reference which is moving with the shock wave. In the new frame of reference the shock speed is zero and the relative velocities are

$$\hat{v}_L = v_L - G_L,\ \hat{v}^* = v^* - G_L . \tag{3.14}$$

In the frame of reference, moving with the shock, the R-H conditions are

$$\rho_L \hat{v}_L = \rho_L^* \hat{v}^* , \tag{3.15}$$

$$\rho_L \hat{v}_L{}^2 + p_L = \rho_L^* \hat{v}^{*2} + p_L^* , \tag{3.16}$$

$$\hat{v}_L (\hat{E}_L + p_L) = \hat{v}^* (\hat{E}_L^* + p^*) . \tag{3.17}$$

Now, introducing the mass flux Q_L which, in view of (3.15) can be written as

$$Q_L = \rho_L \hat{v}_L = \rho_L^* \hat{v}^* . \tag{3.18}$$

From equation (3.16), we have

$$(\rho_L \hat{v}_L)\hat{v}_L + p_L = (\rho_L^* \hat{v}^*)\hat{v}^* + p^* .$$

Using (3.18) in the above equation we obtain

$$Q_L = -\left(p^* - p_L\right) \Big/ \left(\hat{v}^* - \hat{v}_L\right) . \tag{3.19}$$

But $\hat{v}^* - \hat{v}_L = v^* - v_L$.

So, we have

$$Q_L = -\left(p^* - p_L\right) \Big/ \left(v^* - v_L\right) , \tag{3.20}$$

which gives

$$v^* = v_L - \left(p^* - p_L\right)\Big/Q_L\,. \tag{3.21}$$

On substituting the relations $\hat{v}_L = Q_L/\rho_L$, $\hat{v}^* = Q_L/\rho_L^*$, obtained from (3.18) into (3.19) yields

$$Q_L{}^2 = -\left(p^* - p_L\right)\Big/\left(1/\rho_L^* - 1/\rho_L\right). \tag{3.22}$$

Equation (3.17) can be simplified as

$$\hat{v}_L{}^2/2 + \left(e_L + p_L/\rho_L\right) = \hat{v}^{*2}/2 + \left(e_L^* + p^*/\rho_L^*\right). \tag{3.23}$$

Substituting $Q_L = \rho_L^* \hat{v}^*$ and $Q_L = \rho_L \hat{v}_L$ in (3.22), yields the following relations

$$\hat{v}^{*2} = \left(\rho_L/\rho_L^*\right)\left(p_L - p^*\right)\Big/\left(\rho_L - \rho_L^*\right), \tag{3.24}$$

$$\hat{v}_L{}^2 = \left(\rho_L^*/\rho_L\right)\left(p^* - p_L\right)\Big/\left(\rho_L^* - \rho_L\right). \tag{3.25}$$

Using (3.24)-(3.25) in (3.23) and simplifying, we get

$$e_L^* - e_L = (p^* + p_L)\left(\rho_L^* - \rho_L\right)\Big/\left(2\rho_L^*\rho_L\right).$$

Using the equation (3.5) in the above equation, we have

$$\rho_L^*/\rho_L = \left(p^*/p_L + \Pi/(1+\Pi)\right)\Big/\Big(\left(p^*/p_L\right)\left(\Pi + \theta\rho_L\right)\big/\left(1+\Pi\right) + 1 - \theta\rho_L\big/\left(1+\Pi\right)\Big). \tag{3.26}$$

Substituting the value of ρ_L^* in (3.22), we get

$$Q_L = \left[\left(p^* + B_L\right)\Big/A_L\right]^{1/2}, \tag{3.27}$$

where

$$A_L = \left(1 - \theta\rho_L\right)\Big/\left(\rho_L(1+\Pi)\right), \quad B_L = \Pi p_L\Big/\left(1+\Pi\right). \tag{3.28}$$

Thus (3.21) reduces to

$$v^* = v_L - f_L(p^*, V_L), \tag{3.29}$$

where

$$f_L(p^*, V_L) = (p^* - p_L)\left[A_L \big/ \left(p^* + B_L \right) \right]^{1/2}. \qquad (3.30)$$

3.4.2 Left Rarefaction Wave

Suppose that the left wave is a rarefaction wave. The unknown state V_L^* is now connected to the left data state V_L using the isentropic relation and the generalized Riemann invariants for the left wave.

The isentropic law (Pai, 1977)

$$p = A\left(\rho \big/ (1-\theta\rho) \right)^{\Gamma}, \qquad (3.31)$$

where $A = p_L\left(\rho_L \big/ (1-\theta\rho_L) \right)^{-\Gamma}$, may be used across rarefactions.

Applying (3.31) in star region, we get

$$\rho_L^* / \rho_L = \left(\left(p^*/p_L \right)^{1/\Gamma} \big/ (1-\theta\rho_L) \right) \Big/ \left(1 + \left(p^*/p_L \right)^{1/\Gamma} \theta\rho_L \big/ (1-\theta\rho_L) \right). \qquad (3.32)$$

The Riemann invariant across the wave $\lambda_1 = v - c$ is

$v + \int (c/\rho) d\rho =$ constant.

Using $c = \left(\Gamma p \big/ \left(\rho(1-\theta\rho) \right) \right)^{1/2}$, we have

$$v + 2c(1-\theta\rho) \big/ (\Gamma - 1) = \text{constant}. \qquad (3.33)$$

Evaluating the constant on the left data state, we can write

$$v_L + 2c_L(1-\theta\rho_L) \big/ (\Gamma-1) = v^* + 2c_L^*(1-\theta\rho_L^*) \big/ (\Gamma-1), \qquad (3.34)$$

where c_L and c_L^* denote the sound speed on the left and right states bounding the left rarefaction wave. Substituting the value of ρ_L^* from (3.32) into the definition of c_L^*, we have

$$c_L^* = c_L\left(p^*/p_L \right)^{(\Gamma-1)/2\Gamma} (1-\theta\rho_L) \left\{ 1 + \left(p^*/p_L \right)^{1/\Gamma} \theta\rho_L \big/ (1-\theta\rho_L) \right\}. \qquad (3.35)$$

Now, using (3.35) in (3.34), we have

$$v^* = v_L - f_L(p^*, V_L), \tag{3.36}$$

with

$$f_L(p^*, V_L) = 2c_L(1-\theta\rho_L)\big/(\Gamma-1)\left\{\left(p^*/p_L\right)^{(\Gamma-1)/2\Gamma} - 1\right\}. \tag{3.37}$$

3.4.3 Right Shock Wave

Suppose that the right wave is a shock wave travelling with speed G_R. The case may be treated similar to a left shock wave. Here ρ_R, v_R and p_R are values ahead of the shock and ρ_R^*, v^* and p^* are the values behind the shock. In the frame of reference moving with the shock, the shock speed is zero and the relative velocities are

$$\hat{v}_R = v_R - G_R,\ \hat{v}^* = v^* - G_R. \tag{3.38}$$

In the frame of reference moving with the shock, R-H conditions are

$$\rho_R \hat{v}_R = \rho_R^* \hat{v}^*, \tag{3.39}$$

$$\rho_R \hat{v}_R^2 + p_R = \rho_R^* \hat{v}^{*2} + p^*, \tag{3.40}$$

$$\hat{v}_R(\hat{E}_R + p_R) = \hat{v}^*(\hat{E}_R^* + p^*). \tag{3.41}$$

Defining the mass flux as

$$Q_R = -\rho_R \hat{v}_R = -\rho_R^* \hat{v}^*, \tag{3.42}$$

and proceeding similarly, as in the case of left shock wave, we have the density pressure relation as

$$\rho_R^*/\rho_R = \left(p^*/p_R + \Pi/(1+\Pi)\right)\Big/\left(\left(p^*/p_R\right)\left(\Pi + \theta\rho_R\right)/\left(1+\Pi\right) + 1 - \theta\rho_R/\left(1+\Pi\right)\right). \tag{3.43}$$

The mass flux as

$$Q_R = \left[\left(p^* + B_R\right)/A_R\right]^{1/2}, \tag{3.44}$$

with

$$A_R = (1-\theta\rho_R)/(\rho_R(1+\Pi)), \quad B_R = \Pi p_R/(1+\Pi), \tag{3.45}$$

and the particle velocity as

$$v^* = v_R + f_R(p^*, V_R), \tag{3.46}$$

where

$$f_R(p^*, V_R) = (p^* - p_R)\left[A_R/(p^* + B_R)\right]^{1/2}. \tag{3.47}$$

3.4.4 Right Rarefaction Wave

Suppose that the right wave is rarefaction wave. Applying the isentropic law, we get the density pressure relation as

$$\rho_R^*/\rho_R = \left(\left(p^*/p_R\right)^{1/\Gamma}/(1-\theta\rho_R)\right)\Big/\left(1+\left(p^*/p_R\right)^{1/\Gamma}\theta\rho_R/(1-\theta\rho_R)\right), \tag{3.48}$$

and the generalized Riemann invariant for a right rarefaction wave yields

$$v^* - 2c_R^*(1-\theta\rho_R^*)/(\Gamma-1) = v_R - 2c_R(1-\theta\rho_R)/(\Gamma-1), \tag{3.49}$$

where c_R^* and c_R denote the sound speed on the left and right state bounding the right rarefaction fan. Using (3.48) in the definition of c_R^*, we get

$$c_R^* = c_R\left(p^*/p_R\right)^{(\Gamma-1)/2\Gamma}(1-\theta\rho_R)\left\{1+\left(p^*/p_R\right)^{1/\Gamma}\theta\rho_R/(1-\theta\rho_R)\right\}. \tag{3.50}$$

Using (3.50) in (3.49), we get

$$v^* = v_R + f_R(p^*, V_R), \tag{3.51}$$

with

$$f_R(p^*, V_R) = 2c_R(1-\theta\rho_R)/(\Gamma-1)\left\{\left(p^*/p_R\right)^{(\Gamma-1)/2\Gamma} - 1\right\}. \tag{3.52}$$

Now, the functions f_L and f_R have been computed for all four possible wave patterns.

By eliminating v^* from equations (3.29) or (3.36) and (3.46) or (3.51), we get

$$v_L - f_L(p^*, V_L) = v_R + f_R(p^*, V_R),$$

or

$$f(p^*, V_L, V_R) \equiv f_L(p^*, V_L) + f_R(p^*, V_R) + v_R - v_L = 0, \tag{3.53}$$

which is the required equation for pressure. If the nonlinear algebraic equation is solved (analytically or numerically) for p^*, then the solution for particle velocity v^* can be determined from equation (3.29), if left wave is a shock wave $(p^* > p_L)$ or from equation (3.36), if left wave is a rarefaction wave $(p^* \leq p_L)$ or from (3.46), if right wave is a shock wave $(p^* > p_R)$ or from (3.51), if right wave is a rarefaction wave $(p^* \leq p_R)$. It can also be found from a mean value as

$$v^* = (v_L + v_R)/2 + (f_R(p^*) - f_L(p^*))/2\,. \tag{3.54}$$

3.5 Numerical solution

The unknown pressure p^* is obtained by solving the single algebraic equation (3.53). If any of the wave (left or right) is a shock wave, it is not easy to solve (3.53), analytically. It can be seen easily that the function f, given by (3.53), is monotonically increasing and concave downward. Also the behaviour of the pressure function depends on the difference $v_R - v_L$. If this difference is larger than a critical value, it will lead to vacuum in the solution of the Riemann problem. We consider only non-vacuum case. The critical value can be found in terms of initial data. For a positive solution of pressure p^* we must have $f(0) < 0$, i.e.,

$$v_R - v_L < 2c_L(1-\theta\rho_L)\big/(\Gamma-1) + 2c_R(1-\theta\rho_R)\big/(\Gamma-1), \tag{3.55}$$

which is the required pressure positivity condition.

Here, the Newton-Raphson iterative procedure is used to find the root of the pressure equation, which is

$$p_{n+1} = p_n - f(p_n)\big/ f'(p_n),$$

where p_n is nth iterate. The iteration procedure is stopped when the relative pressure change $2\left|p_{n+1}-p_n\right|/\left[p_{n+1}+p_n\right]$ is less than a prescribed tolerance (TOL) say 10^{-6}.

To implement the iteration scheme we need a guess value p_0 for pressure. One such approximation is the so called two – Rarefaction approximation (Toro, 2009)

$$p_{TR}=\left[\frac{c_L(1-\theta\rho_L)+c_R(1-\theta\rho_R)-(\Gamma-1)(v_R-v_L)/2}{c_L(1-\theta\rho_L)/(p_L)^{(\Gamma-1)/2\Gamma}+c_R(1-\theta\rho_R)/(p_R)^{(\Gamma-1)/2\Gamma}}\right]^{2\Gamma/(\Gamma-1)}. \tag{3.56}$$

A second guess value can be taken as the Primitive Variable Riemann Solver (PVRS) (Toro, 2009)

$$\left.\begin{array}{l} p_0=\max(TOL,p_{PV}) \\ p_{PV}=(p_L+p_R)/2+(\rho_L+\rho_R)(c_L+c_R)(v_L-v_R)/8 \end{array}\right\}. \tag{3.57}$$

A third guess value is given by a two shock approximation (Toro, 2009)

$$\left.\begin{array}{l} p_0=\max(TOL,p_{TS}) \\ p_{TS}=\left(g_L(\overline{p})p_L+g_R(\overline{p})p_R-(v_R-v_L)\right)\Big/\left(g_L(\overline{p})+g_R(\overline{p})\right) \\ g_K(p)=\left[A_K\big/\left(p+B_K\right)\right]^{1/2} \end{array}\right\}, \tag{3.58}$$

where A_K and B_K are given in equation (3.12). Here $\overline{p}$ is an estimate of the solution.

As a fourth guess value, we can use the arithmetic mean of the data, namely

$$p_0=(p_L+p_R)/2. \tag{3.59}$$

3.6 Summary of the solution

3.6.1 Left Shock Wave

Here a left shock wave is identified by the condition $p^*>p_L$. The values p^*, v^* and ρ_L^* have been calculated. The shock speed G_L is also a function of pressure p^*. From (3.14) and (3.18), we have

$$G_L = v_L - Q_L / \rho_L, \tag{3.60}$$

where Q_L is given by (3.27).

More explicitly, we have

$$G_L = v_L - \left[\left(p^* + B_L\right)/A_L\right]^{1/2} \Big/ \rho_L. \tag{3.61}$$

Thus, if the left wave is a shock wave then the complete solution for the entire region to the left of contact discontinuity has been found.

3.6.2 Left Rarefaction Wave

Also the left rarefaction wave is identified by the condition $p^* \le p_L$. The pressure p^*, particle velocity v^* and density ρ_L^* in the star region have been calculated. The rarefaction wave is consist of the head and tail which are the characteristics of the speed given respectively by

$$G_{HL} = v_L - c_L,\; G_{TL} = v^* - c_L^*. \tag{3.62}$$

Now, the solution for $U_{Lfan} = (\rho, v, p)^T$ inside the left rarefaction fan is computed, which is obtained by considering the characteristic ray through the origin $(0,0)$ and a general point (x,t) inside the fan. The slope of the characteristic is given as

$$dx/dt = x/t = v - c,$$

where v and c are respectively the sought particle velocity and sound speed at (x,t).

Also, use of generalized Riemann invariant yields

$$v_L + 2c_L(1-\theta\rho_L)/(\Gamma-1) = v + 2c(1-\theta\rho)/(\Gamma-1).$$

The solution of these two simultaneous equations is

$$v = \left(v_L + 2c_L(1-\theta\rho_L)/(\Gamma-1) + 2\left(x/t\right)(1-\theta\rho)/(\Gamma-1)\right)\Big/\left(1+2(1-\theta\rho)/(\Gamma-1)\right). \tag{3.63}$$

Also from (3.36), we have

$$v = v_L - 2c_L(1-\theta\rho_L)\big/(\Gamma-1)\left\{\left(p^*/p_L\right)^{(\Gamma-1)/2\Gamma}-1\right\}. \tag{3.63a}$$

From equation (3.63) and (3.63a), we get

$$F(p,\ x/t) = 0, \tag{3.64}$$

where

$$F(p,\ x/t) = \left(\theta\rho_L\big/(1-\theta\rho_L)\right)p^{(\Gamma+1)/2\Gamma} + p_L^{1/\Gamma}\,p^{(\Gamma-1)/2\Gamma}\,(\Gamma+1)\big/(\Gamma-1)$$

$$-p_L^{(\Gamma+1)/2\Gamma}\left\{2\big/(\Gamma-1)+\left(v_L - x/t\right)\big/\left(c_L\left(1-\theta\rho_L\right)\right)\right\}, \tag{3.64a}$$

which is a function of pressure distribution in a left rarefaction fan. It can be easily seen that for a fixed (x,t), we have $F_p > 0$, which shows that F is a monotonically increasing function of pressure. For pressure to be positive, we must have $F\left(0, x/t\right) < 0,$ which gives the pressure positivity condition in the left rarefaction fan given as $\left(2c_L(1-\theta\rho_L)\big/(\Gamma-1)+v_L\right) > x/t$.

Also, for a fixed (x,t), we have $F_{pp} < 0$, which shows that F is a concave downward function of pressure. We can apply the Newton-Raphson iterative procedure to find the root of the pressure equation. An initial approximation is given by equations (3.56), (3.57) or (3.58).

Using equation (3.64), pressure at (x,t) can also be approximated as

$$p/p_L = \left[\left(2\big/(\Gamma-1)+(v_L - x/t)\big/(c_L(1-\theta\rho_L))\right)\Big/\left(\left(\overline{p}/p_L\right)^{1/\Gamma}\theta\rho_L\big/(1-\theta\rho_L)+(\Gamma+1)\big/(\Gamma-1)\right)\right]^{2\Gamma/(\Gamma-1)}, \tag{3.65}$$

where $\overline{p}$ is an approximation to the root of the function given by equation (3.64) and can be taken from any of (3.56), (3.58) or (3.59).

Once the pressure at point (x,t) has been calculated, density at that point may be given by (3.32), which is

$$\rho/\rho_L = \left(\left(p/p_L\right)^{1/\Gamma} \big/ (1-\theta\rho_L)\right) \Big/ \left(1 + \left(p/p_L\right)^{1/\Gamma} \theta\rho_L \big/ (1-\theta\rho_L)\right). \tag{3.66}$$

Finally, the velocity at (x,t) is given by (3.63).

3.6.3 Right Shock Wave

A right shock wave is identified by the condition $p^* > p_R$. The values p^*, v^* and ρ_R^* have been calculated. The shock speed is

$$G_R = v_R + Q_R / \rho_R, \tag{3.67}$$

where Q_R is given by (3.44). More explicitly, we have

$$G_R = v_R + \left[\left(p^* + B_R\right)/A_R\right]^{1/2} \Big/ \rho_R \,. \tag{3.68}$$

Thus, if the right wave is a shock wave then the complete solution for the entire region to the right of contact discontinuity has been found.

3.6.4 Right Rarefaction Wave

The solution procedure is entirely analogous to the case of left rarefaction wave. A right rarefaction wave is identified by the condition $p^* \le p_R$. The pressure p^*, particle velocity v^* and density ρ_R^* in the star region have been calculated. The rarefaction wave is enclosed by the head and tail which are the characteristics of the speed given respectively by

$$G_{HR} = v_R + c_R,\ G_{TR} = v^* + c_R^*. \tag{3.69}$$

We now determine the solution for $U_{Rfan} = (\rho, v, p)^T$ inside the right rarefaction fan. This is easily obtained by considering the characteristic ray through the origin $(0,0)$ and a general point (x,t) inside the fan. The slope of the characteristic is

$$dx/dt = x/t = v + c\ ,$$

where v and c are respectively the sought particle velocity and sound speed at (x,t) .

Also, use of generalized Riemann invariant yields

$$v - 2c(1-\theta\rho)/(\Gamma - 1) = v_R - 2c_R(1-\theta\rho_R)/(\Gamma - 1).$$

The solution of these two simultaneous equations is

$$v = \left(v_R - 2c_R(1-\theta\rho_R)/(\Gamma-1) + 2(x/t)(1-\theta\rho)/(\Gamma-1)\right)/\left(1 + 2(1-\theta\rho)/(\Gamma-1)\right). \tag{3.70}$$

Also from (3.51), we have

$$v = v_R + 2c_R(1-\theta\rho_R)/(\Gamma-1)\left\{\left(p^*/p_R\right)^{(\Gamma-1)/2\Gamma} - 1\right\}. \tag{3.70a}$$

From equation (3.70) and (3.70a), we get

$$F(p, x/t) = 0, \tag{3.71}$$

where

$$F(p,\ x/t) = \theta\rho_R p^{(\Gamma+1)/2\Gamma}/(1-\theta\rho_R) + p_R^{1/\Gamma} p^{(\Gamma-1)/2\Gamma}(\Gamma+1)/(\Gamma-1)$$
$$+ p_R^{(\Gamma+1)/2\Gamma}\left\{-2/(\Gamma-1) + (v_R - x/t)/\left(c_R(1-\theta\rho_R)\right)\right\}, \tag{3.71a}$$

which is a function for distribution of pressure in right rarefaction fan. It can be easily seen that for a fixed (x,t), we have $F_p > 0$, which shows that F is a monotonically increasing function of pressure. For pressure to be positive, we must have $F(0, x/t) < 0$, which gives the pressure positivity condition in the right rarefaction fan as $\left(v_R + 2c_R(1-\theta\rho_R)/(\Gamma-1)\right) < x/t$.

Also, for a fixed (x,t), we have $F_{pp} < 0$, which shows that F is a concave downward function of pressure. The Newton-Raphson iterative procedure is applied to find the root of the pressure equation. An initial approximation is given by equation (3.56), (3.57), or (3.58).

Using equation (3.71), pressure at (x,t) can also be approximated as

$$p/p_R = \left[\left(2/(\Gamma-1) - (v_R - x/t)/(c_R(1-\theta\rho_R))\right)\Big/\left(\left(\bar{p}/p_R\right)^{1/\Gamma}\theta\rho_R/(1-\theta\rho_R) + (\Gamma+1)/(\Gamma-1)\right)\right]^{2\Gamma/(\Gamma-1)}, \quad (3.72)$$

where $\bar{p}$ is an approximation to the root of the function given by equation (3.71) and can be taken from any of (3.56), (3.58) or (3.59).

Once the pressure at point (x,t) has been calculated, density at that point be given by (3.48), which is

$$\rho/\rho_R = \left(\left(p/p_R\right)^{1/\Gamma}/(1-\theta\rho_R)\right)\Big/\left(1+\left(p/p_R\right)^{1/\Gamma}\theta\rho_R/(1-\theta\rho_R)\right). \quad (3.73)$$

Finally, the velocity at (x,t) is given by (3.70).

3.7 Result and discussion

All we need is an appropriate value of θ, to assess the effect of dust particles on the solution profiles. Since $\theta = Z/\rho$ and θ is constant, we must have $\theta = Z_L/\rho_L = Z_R/\rho_R$. Consider a dusty gas with density ρ_1, pressure p_1 and volume V_1. The volume fraction of the mixture is Z_1 and mass fraction k_p, we have $\theta = Z_1/\rho_1 = (V_{sp}/V_1)/\rho_1$. When the mixture is compressed up to a pressure p_2, the density and volume is taken as ρ_2 and V_2 respectively. The mass fraction k_p remains constant but the volume fraction becomes $Z_2 = \theta\rho_2$. By the conservation of mass, $\rho_1 V_1 = \rho_2 V_2$. Therefore $\theta = Z_2/\rho_2 = (V_{sp}/V_2)/(\rho_1 V_1/V_2) = (V_{sp}/V_1)/\rho_1 = Z_1/\rho_1$. Thus, the value of θ is to be chosen such that the volume fraction $Z = V_{sp}/V_g$ on the left and right data is less than 5%. For a given value of Z, an obvious choice is $\theta = Z/\rho_K$, where $\rho_K = \max(\rho_L, \rho_R)$.

Five test problems are selected to check the applicability of the method for the dusty gas flow. In test 1, the solution profile for dusty gas is compared with that of ideal gas without dust particle. In test 2-5, the solution profile for the case of dusty gas flow is plotted. The data for all five tests in terms of primitive variables for dusty gas is shown in the table 1 given below.

Test	ρ_L	v_L	p_L	ρ_R	v_R	p_R
1	1.0	0.0	1.0	0.125	0.0	0.1
2	1.0	-2.0	0.4	1.0	2.0	0.4
3	1.0	0.0	1000.0	1.0	0.0	0.01
4	1.0	0.0	0.01	1.0	0.0	100.0
5	5.99924	19.5975	460.894	5.99242	-6.19633	46.0950

Table 3.1: Data for test problems

Test 1 is the Sod test problem (1978). Its solution results in a left rarefaction, a contact and a right shock. Figures 3.2 – 3.13 shows the solution profile in the case of dusty gas with different values of mass fraction, specific heat and volume fraction of solid particles. Test 2 is called the 123 problem given in Toro (2009), has solutions consisting of two strong rarefactions and a stationary contact discontinuity and figures 3.14 (a) – (d) show the solution profiles. Test 3 is the left half of the blast wave problem of Woodward and Colella (1984). Its solution consists of a left rarefaction, a contact and a right shock and figures 3.15 (a) – (d) show the corresponding solution profiles. Test 4 is the right half of the Woodward and Colella problem. Its solution consists of a left shock, a contact and a right rarefaction and figures 3.16 (a) – (d) show the solution profiles. Test 5 consists of shock solutions of test 3 and test 4 for ordinary gas dynamics. Its solution consists of a left shock, a contact discontinuity and a right shock wave and figures 3.17 (a) – (d) show the solution profiles.

In all cases the ratio of specific heats is $\gamma = 1.4$.

Figures 3.2 – 3.5 show the solution profiles for density, velocity, pressure and internal energy respectively for different values of mass fraction, at $Z = 0.01, \beta = 0.5$. Figures 3.6 – 3.9 show the solution profiles for different values of specific heat of solid particles, when $Z = 0.01, k_p = 0.3, \lambda = 0.4286$. Figures 3.10 – 3.13 show the solution profiles for different values of volume fraction when $\beta = 0.8, k_p = 0.3, \lambda = 0.4286$.

In figures 3.2 – 3.13, the case $Z = 0.0$, corresponds to ordinary gasdynamics and are identical to those obtained in Toro (2009). The Figures show that the effect of increasing values of the parameters of dust particles is to reduce the length of star region. From figures 3.2 – 3.5 it can be inferred that an increase in the value of mass fraction causes the head of the rarefaction wave to move faster, the contact discontinuity to become weaker and the shock wave to become stronger as compared to ordinary gasdynamics case. The effects obtained in solution profiles is due to the reason that any increase in the k_p or β causes the Grüneisen coefficient Γ to decrease which results in a general rise of density, velocity etc. in the star region relative to what it would be in the absence of dust particles and this causes to shrink the star region.

Figures 3.6 – 3.9 show that by increasing the specific heat of solid particles a similar behaviour is observed as for the case of corresponding figures 3.2 – 3.5, which is expected.

Figures 3.10 – 3.13 show that the effect of an increase in the value of volume fraction also produces similar behaviour in nature with reduced magnitude as compared to the above corresponding cases of figures 3.2 – 3.9.

From figures 3.2 – 3.13, it can be concluded that the solution profiles in case of dusty gas depends solely on the nature of dust particles i.e., mass fraction, volume fraction and specific heat of solid particles.

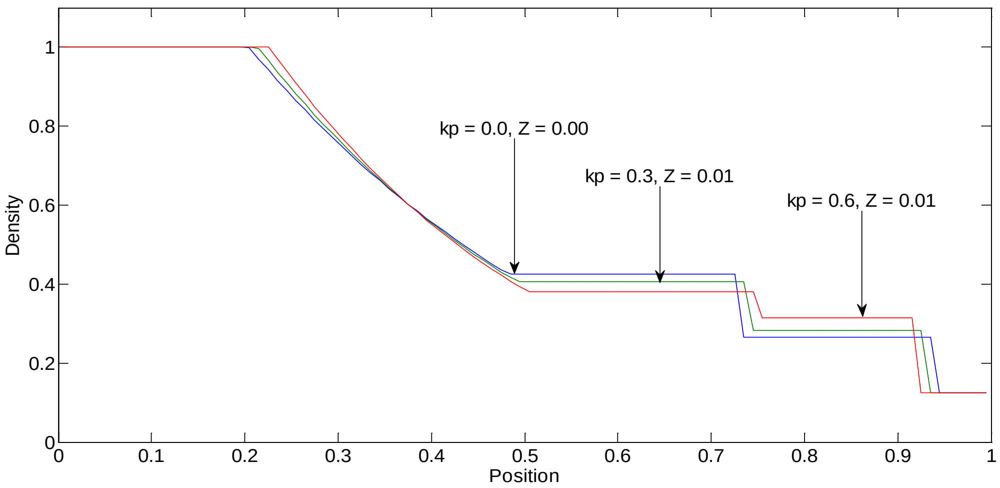

Figure 3.2 Density profile

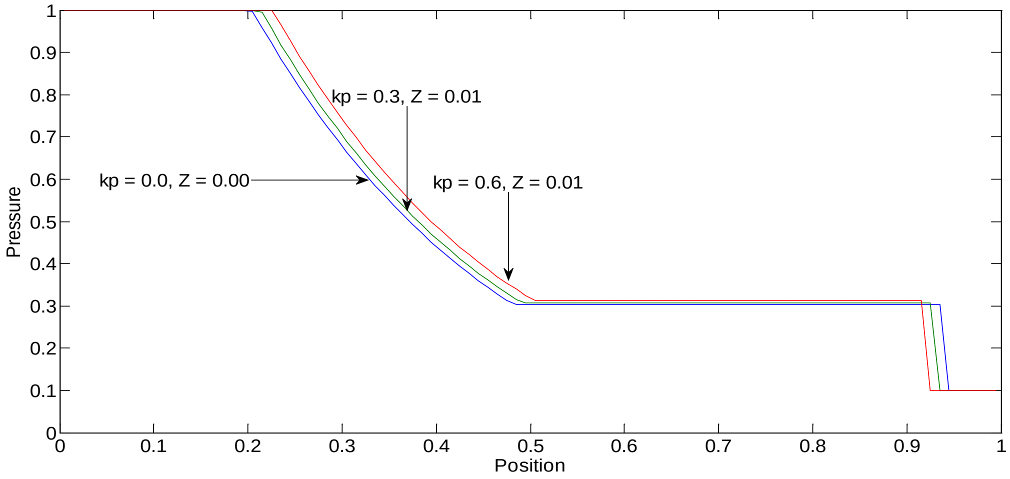

Figure 3.3 Pressure profile

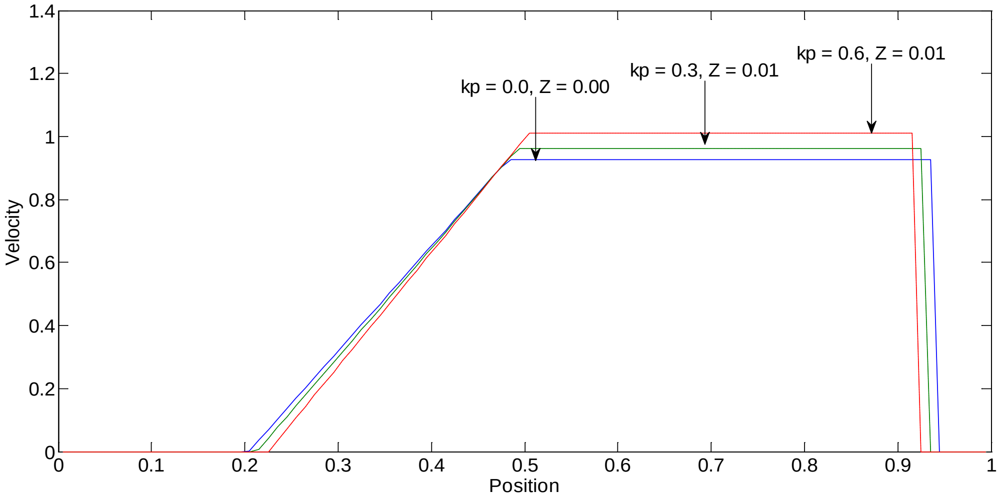

Figure 3.4 Velocity profile

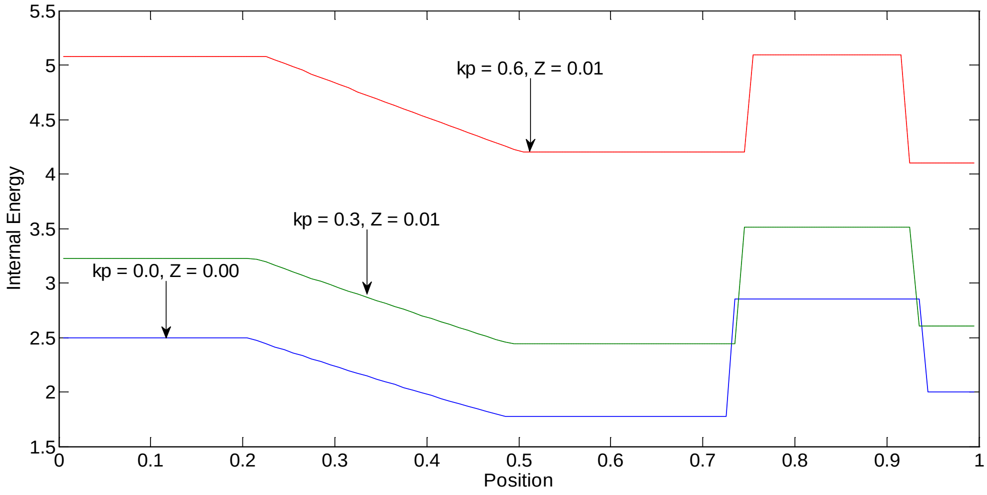

Figure 3.5 Internal Energy profile

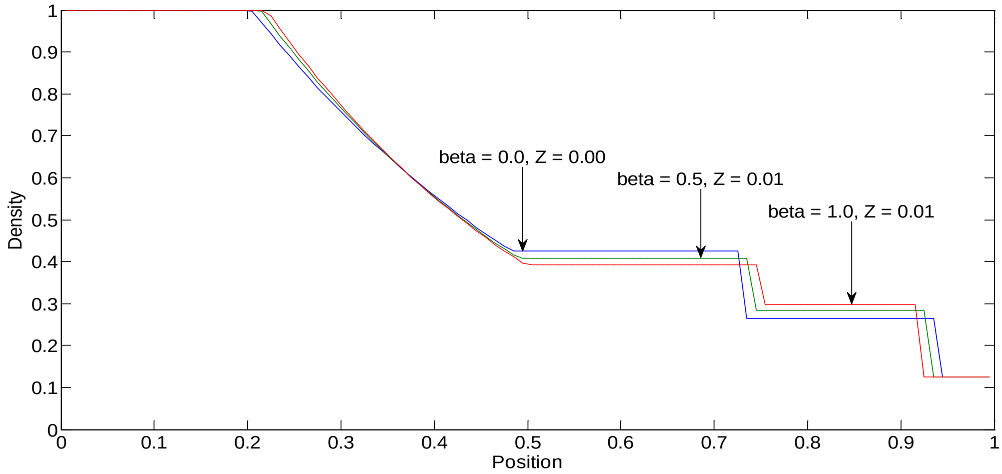

Figure 3.6 Density profile

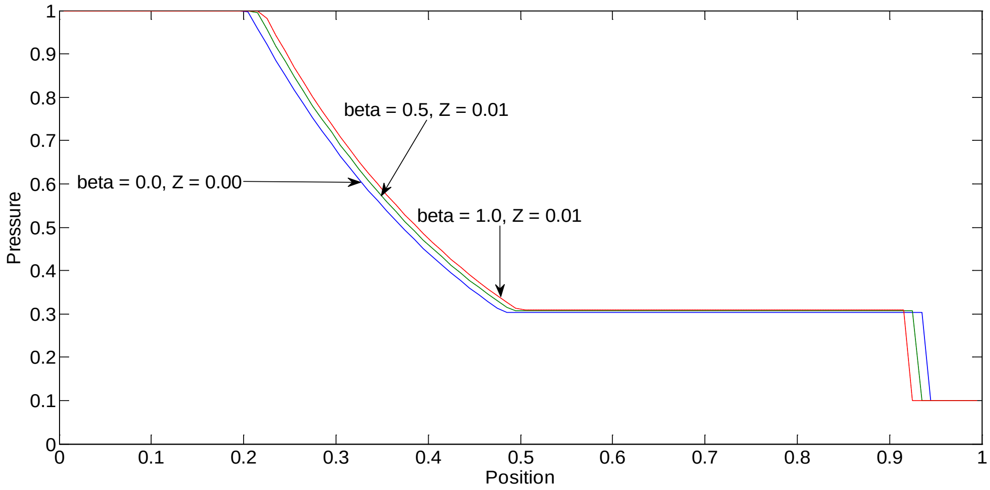

Figure 3.7 Pressure profile

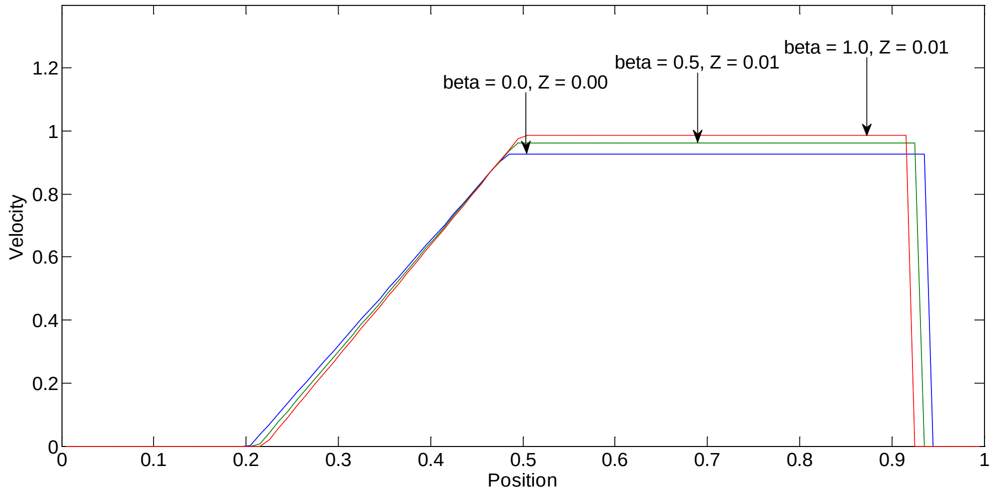

Figure 3.8 Velocity profile

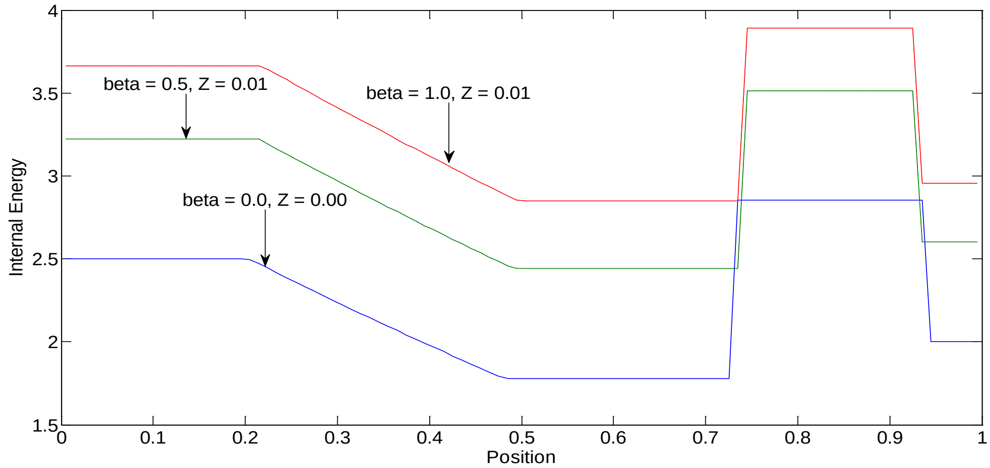

Figure 3.9 Internal Energy profile

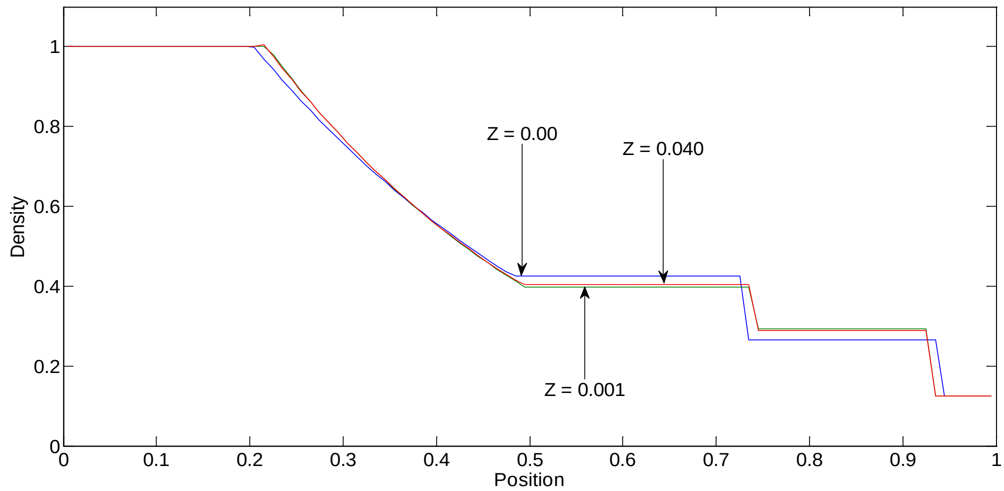

Figure 3.10 Density profile

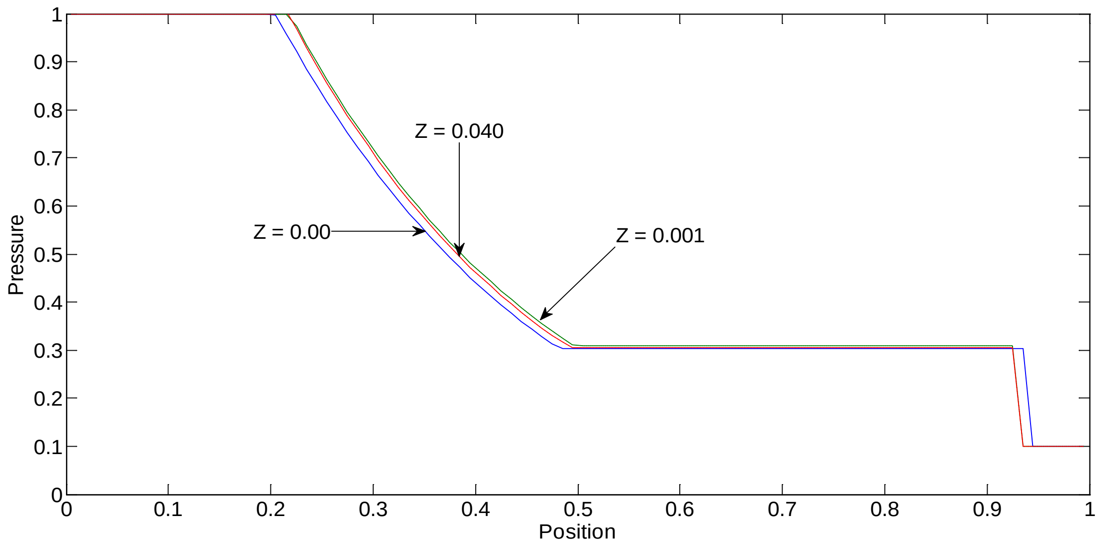

Figure 3.11 Pressure profile

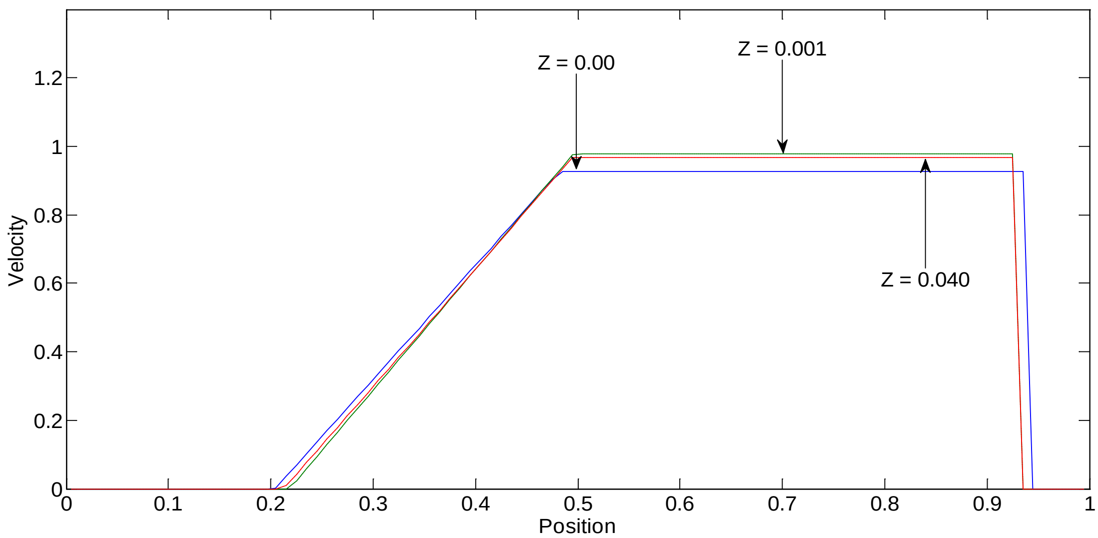

Figure 3.12 Velocity profile

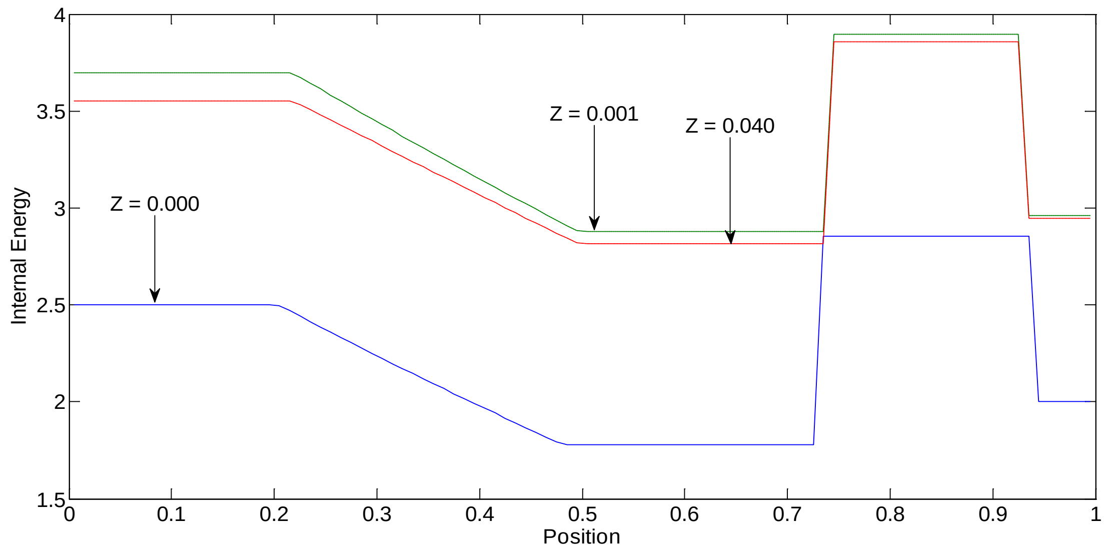

Figure 3.13 Internal Energy profile

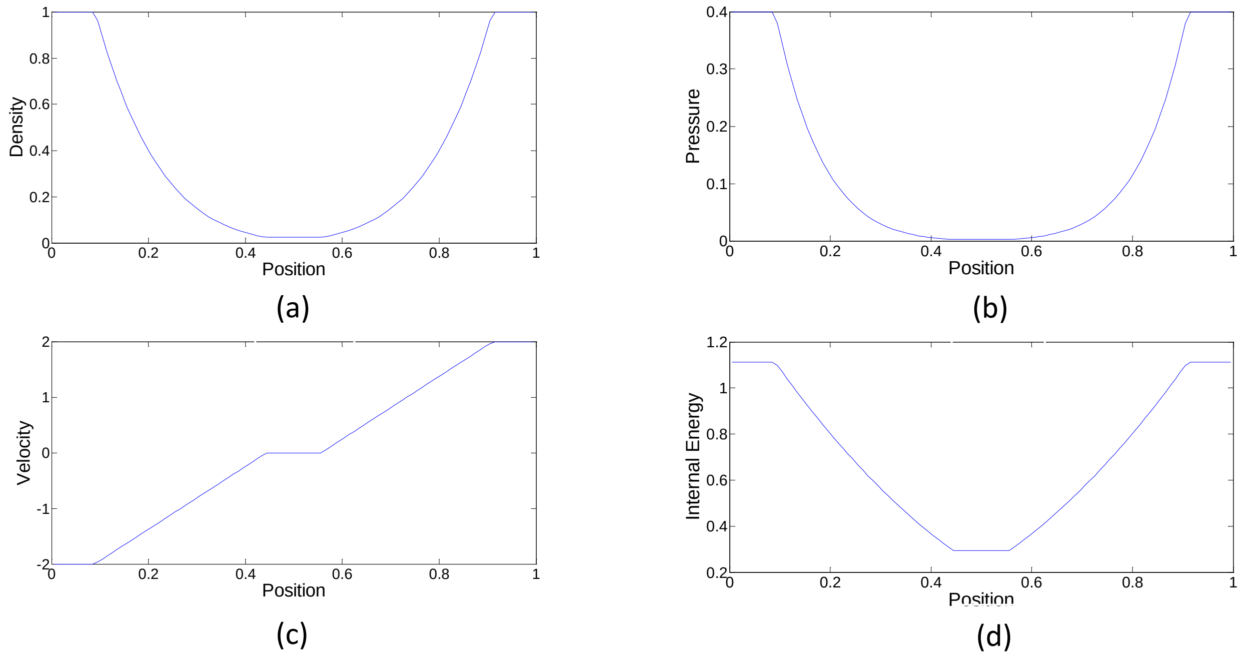

Figures 3.14 (a) – (d) Solution profiles for **Test 2**; $k_p = 0.1$, $\lambda = 0.1111$, $\beta = 0.8$, $\theta = 0.01$. at $t = 0.15s$

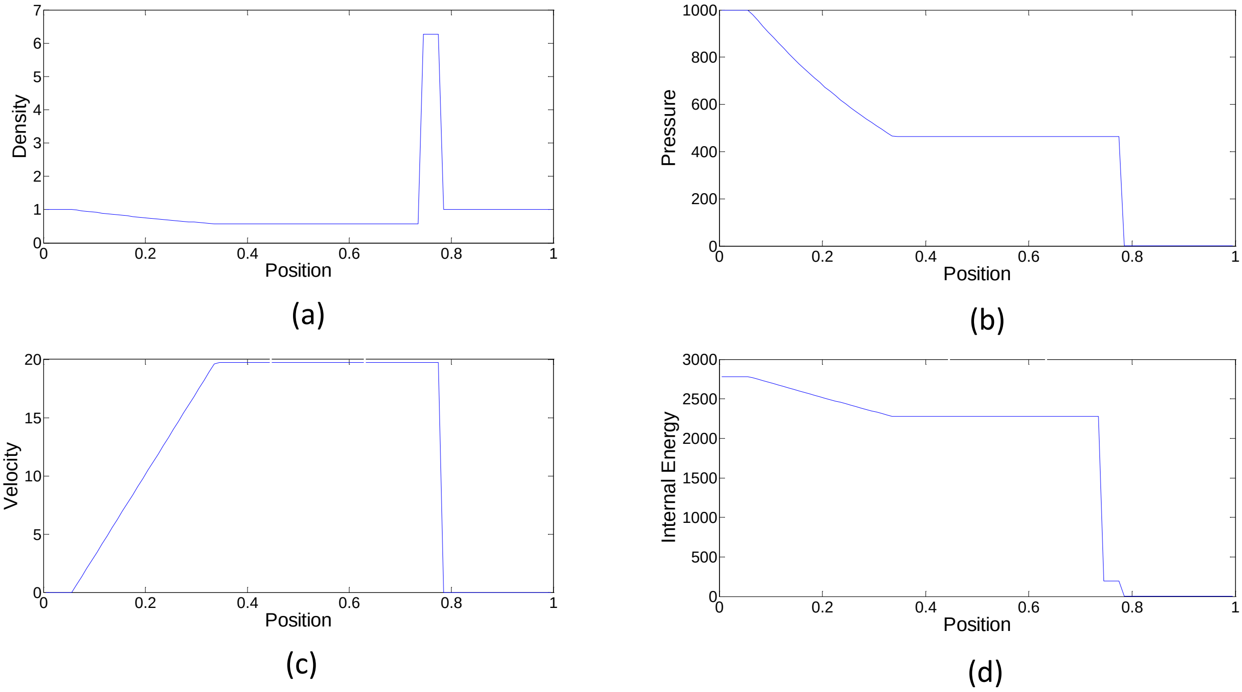

Figures 3.15 (a) – (d) Solution profiles for **Test 3**; $k_p = 0.1$, $\lambda = 0.1111$, $\beta = 0.8$, $\theta = 0.01$ at time $t = 0.012s$.

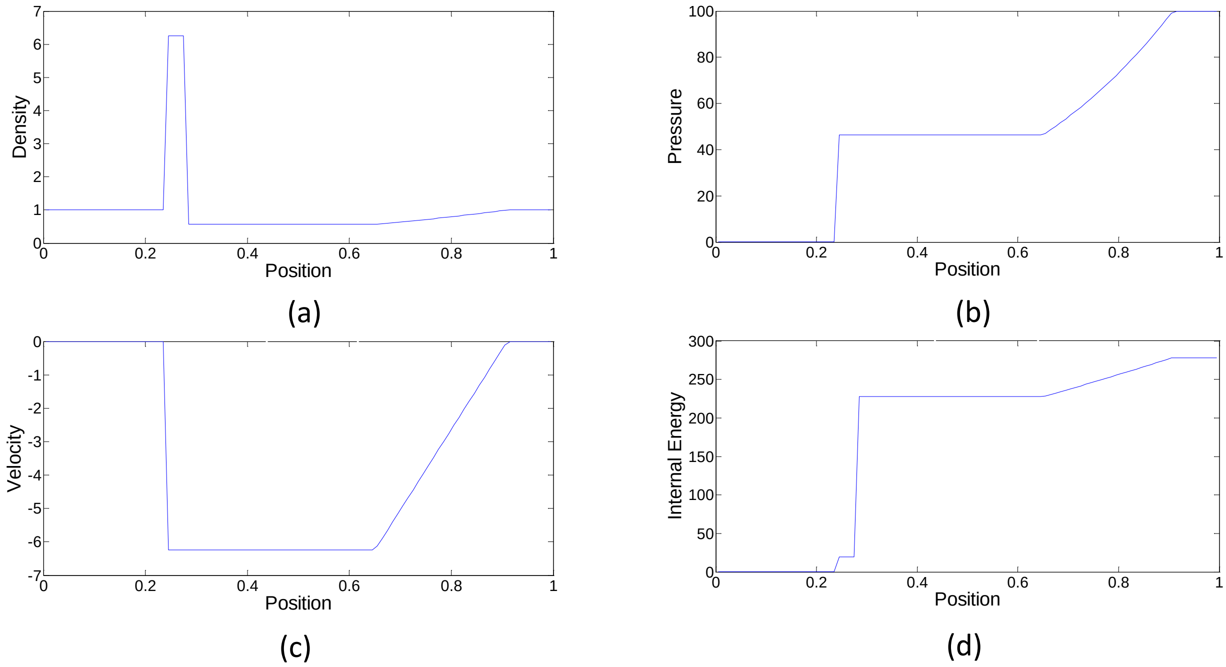

Figures 3.16 (a) – (d) Solution profiles for **Test 4;** $k_p = 0.1$, $\lambda = 0.1111$, $\beta = 0.8$, $\theta = 0.01$ at time $t = 0.035s$.

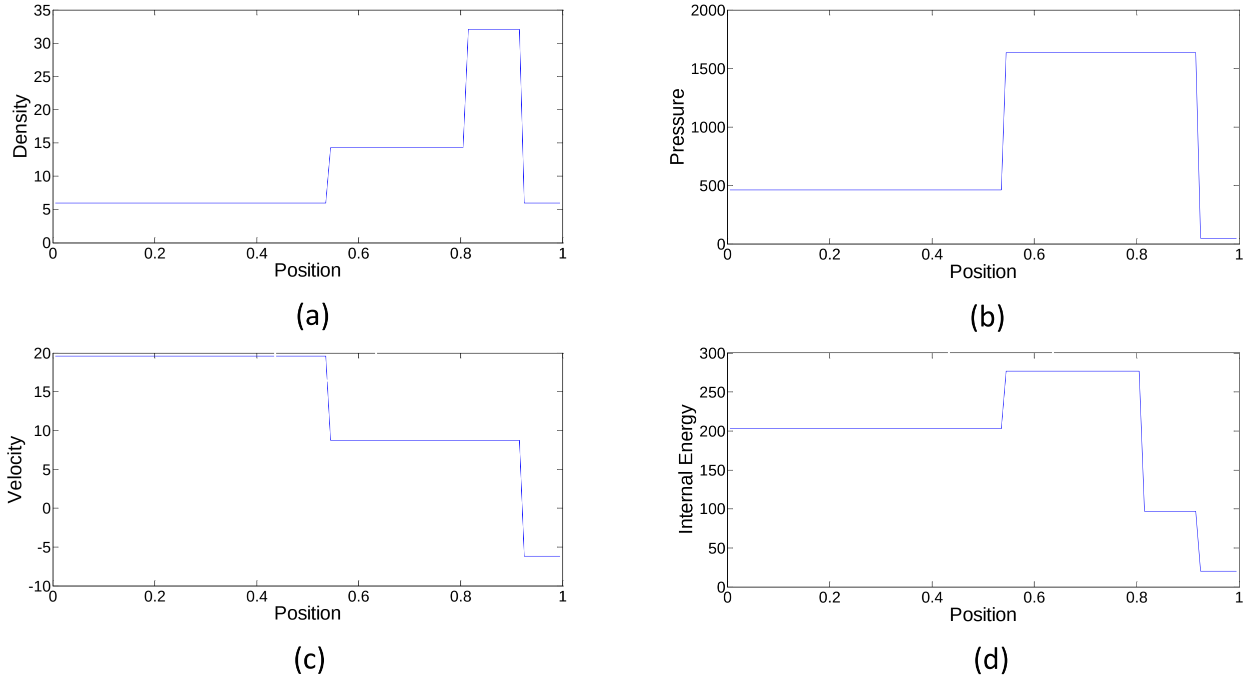

Figures 3.17 (a) – (d) Solution profiles for **Test 5**; $k_p = 0.1$, $\lambda = 0.1111$, $\beta = 0.8$ $\theta = 0.001667$ at time $t = 0.035s$.